Research Concerning the Interaction between the Ground and the Turbulent Aircraft Wake Vortex

Dan RĂDUCANU, Ion NEDELCU,
Doru SAFTA, Cristian-Emil MOLDOVEANU, Pamfil ŞOMOIAG

***Abstract*—The problem developed in this contribution is encountered in airplane aerodynamics and concerns the influence of long life longitudinal wake vortices generated by wing tips or by external obstacles such as reactors or landing gears. More generally it concerns 3D bodies of finite extension in cross flow. At the edge of such obstacles, longitudinal vortices are created by pressure differences inside the boundary layers and rotate in opposite senses. The numerical simulation used for understanding the mechanisms were generally time evolution computation on a fixed space box with periodic boundary conditions using a transformation of the time evolution into a downstream evolution. The flow will be perturbed by prescribed disturbances or by a turbulent field.**

***Index Terms* -Aircraft, Wake Vortex, Large Eddy Simulation, Ground Effect, Enstrophy, Vorticity**

I. Introduction

The vortex mechanisms intervene in a great number of flows and in various forms. In the aeronautical mediums, we can meet vortices which can be of very different scales. Any object moving in the air leaves behind a more or less organized wake. In case of an aircraft, this wake vortex results in a rolling up of the flow starting from the ends of the wings (fig.1). The aircraft wake vortex can be described by two main counter-rotating vortices. It is due to the lift of each wing and the generated vortices will be all more intense as this lift will be large.

When atmospheric conditions are favorable to the condensation, or when the plume of smoke generated by the reactors comes to mingle with the vortices, we can notice the trace of these vortices in the sky. These vortices have a life that can be quite long. The biggest problem relates to the risk of incidents caused by the meeting of an aircraft with a turbulent wake vortex generated by another aircraft that preceded it. This problem is more important in the phases of takeoff and landing (Fig. 1), where the aircrafts are allowed to follow at a rate close, and where the ground proximity may produce such disastrous incidents.

Fig. 1 Aircraft Wake Vortex

Vortex decay near the ground is known to be enhanced by proximity to the ground, but details are not well understood. For aircraft wake vortices away from the ground, ambient atmospheric turbulence has been recognized to be a key factor for the enhancement of the vortex decay [3]. At low altitudes, however, the interaction of the vortices with the ground may be a more important factor for vortex decay.

The aim of this work is to study the vorticity generation for a counter-rotating vortices pair in the ground effect. A three-dimensional numerical Large Eddy Simulation is used.

II. Generation of the Vorticity at the Wall

The concept of vorticity flux has been introduced by Lighthill in 1963. The algorithm generates particles of vorticity at the wall by evaluating at each time step the flux of vorticity (see Cottet and Koumoutsakos for details [6]). The concept is analog to the Fourier law for the heat flux. We explain this concept in a 2D situation but this can be extended to 3D.

At a plane solid wall extended along Ox axis with normal Oy, the mechanical equilibrium of a fluid particle in projection tangent to the wall writes as:

Manuscript received the 23 March, 2009. This work was supported in part by the Romanian Space Agency and Military Technical Academy.

D. Răducanu is with Technical College for Defense and Security, Military Technical Academy, No. 81-83, Avenue George Coşbuc, Sector 5, Bucharest, Romania, and with Romanian Space Agency (ROSA), No. 21-25 Avenue Mendeleev, Sector 1, Bucharest, Romania, phone:+40.722.229.547, fax: +40.213.355.763, e-mail: dan.raducanu@rosa.ro;

I. Nedelcu is with Romanian Space Agency (ROSA), No. 21-25 Avenue Mendeleev, Sector 1, Bucharest, Romania, phone: +40.213.168.722, fax: +40.213.128.804, e-mail: ion.nedelcu@rosa.ro;

D. Safta is with the Mechatronics Department, Military Technical Academy, No. 81-83, Avenue George Coşbuc, Sector 5, Bucharest, cod 050141, Romania, phone: +40.213.354.660, fax: +40.213.355.763, e-mail: dsafta@mta.ro;

C.E. Moldoveanu is with the Mechatronics Department, Military Technical Academy, No. 81-83, Avenue George Coşbuc, Sector 5, Bucharest, cod 050141, Romania, phone: +40.721.288.312, fax: +40.213.355.763, e-mail: mcrristi@gmail.com;

P. Şomoiag is with the Mechatronics Department, Military Technical Academy, No. 81-83, Avenue George Coşbuc, Sector 5, Bucharest, cod 050141, Romania, phone: +40.723.173.300, fax: +40.213.355.763, e-mail: somoiag.pamfil@gmail.com.

$$-\frac{\partial p}{\partial x}\bigg|_{wall}+\mu\frac{\partial^2 u}{\partial y^2}\bigg|_{wall}=0, \qquad (1)$$

along with the vorticity at the wall:

$$\omega_z=-\frac{\partial u}{\partial y}\bigg|_{wall}. \qquad (2)$$

Combining these two relations we obtain φ_ω the vorticity flux:

$$\varphi_\omega=-\mu\frac{\partial \omega}{\partial y}\bigg|_{wall}=\frac{\partial p}{\partial x}\bigg|_{wall}. \qquad (3)$$

A classical illustration of the concept is the separation of a boundary layer when a positive pressure gradient leads to a positive flux of vorticity and correspond to the injection in the flow of a positive amount of vorticity that increases the value of $\omega_z|_{wall}$ to zero.

When a coherent vortex structure moves close to a wall, the inviscid potential theory of point vortices and the second unsteady Bernoulli's theorem are two efficient tools for evaluating the pressure at the wall and then the vorticity flux [7]. As an example the case of two counter-rotating equal vortices (fig. 2) can be presented [5].

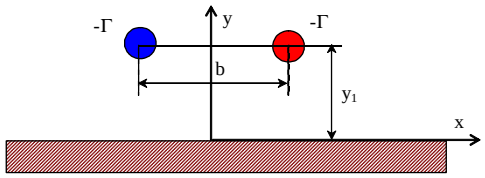

Fig. 2 The generation of the wake vortex

The trajectory of these vortices (±Γ) initially at $\pm x_1=\pm b/2$, y_1 are described by:

$$\frac{1}{x^2}+\frac{1}{y^2}=\frac{1}{x_1^2}+\frac{1}{y_1^2}. \qquad (4)$$

At the beginning we have an impact effect on the wall with a vertical velocity to the wall followed by a sweeping effect with a tangential velocity of the vortices.

The pressure is then evaluated through the relation at the wall:

$$p(x)+\frac{1}{2}\rho_0 V_{wall}^2+\rho_0\frac{\partial\varphi}{\partial t}=p_0, \qquad (5)$$

were φ is the velocity potential and V_{wall} the velocity obtained by considering the counter-rotating point vortices and their images relative to the wall.

Straightforward calculations give the expressions:

$$V_{wall}^2=\frac{16\Gamma^2}{\pi^2}\left[\frac{xx_1y_1}{B}\right]^2, \qquad (6)$$

$$\frac{\partial\varphi}{\partial t}\bigg|_{wall}=\frac{\Gamma^2}{2\pi^2}\frac{1}{x_1^2+y_1^2}\frac{A}{B}, \qquad (7)$$

where:

$$A=x^2\left(y_1^2-x_1^2\right)-\left(x_1^2+y_1^2\right)^2, \qquad (8)$$

$$B=\left(x^2+x_1^2+y_1^2\right)^2-4x^2x_1^2. \qquad (9)$$

And finally the pressure distribution at the wall is described by the relation:

$$p(x)-p_0=-\frac{\rho_0\Gamma^2}{2\pi^2}\left[\left(\frac{4xx_1y_1}{B}\right)^2+\frac{1}{x_1^2+y_1^2}\frac{A}{B}\right]. \qquad (10)$$

The figures 3 and 4 shows the pressure distributions and the corresponding vorticity flux for the impact and sweeping situations along with the position of the vortex on its trajectory.

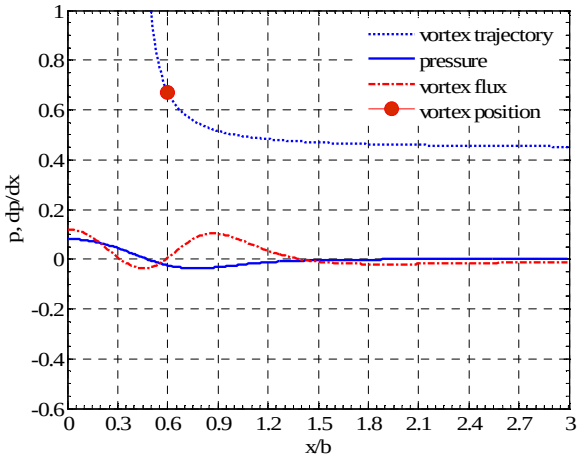

Fig. 3 The pressure distribution and the vorticity at the wall for the impact situation

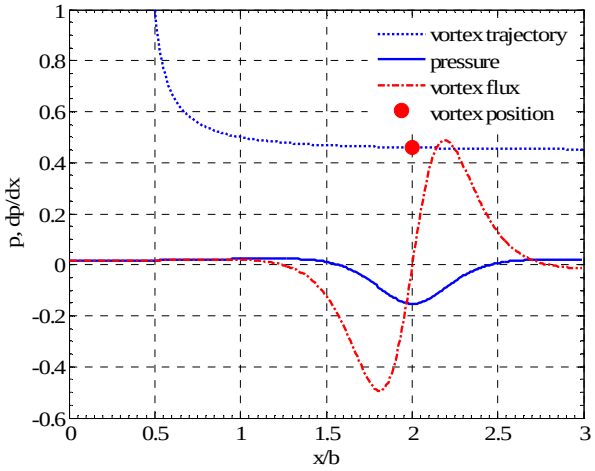

Fig. 4 The pressure distribution and the vorticity at the wall for the sweeping situation

It can be observed that each vortex produces negative and positive vorticity at the wall. For the impact situation (fig. 3) the vorticity flux is mainly on opposite sign compared to the vortex, for the sweeping situation the two signs of vorticity are present.

III. Numerical Tools and Physical Model

In order to study the influence of the ground at a counter-rotating vortices pair we use a numerical simulation based on a Large Eddy Simulation computing code with a sub-grid model. The three dimensional version having been fully described by Calmet and Magnaudet [4], we present here a summary of the numerical method.

The momentum and scalar equations are discretized using a second-order accurate centered schemes on a staggered grid. The resulting terms are integrated in space on finite volumes and the solution is advanced in time by means of a three-step Runge-Kutta time steeping procedure [1]. The non linear terms of each equation are computed explicitly while the diffusive terms are calculated using the semi-implicit Crank-Nicholson algorithm. To satisfy the incompressibility condition, a Poisson equation is solved by combining a direct inversion in the (x,y) plane with a spectral Fourier method in the z direction. The use of a spectral Fourier method implying periodicity increases the accuracy and the rapidity of the code.

The main idea of the Large Eddy Simulation is to consider that integrality of turbulent agitation ceases being random. Thus, the contributions to the large scales are explicitly calculated, modeling being reserved for the structures whose size is lower than a dimension characteristic of the mesh of computation.

The advantage of this method is to reduce the two deficiencies of the other methods: empiricism of one-point closure of the averaged equations and requirement in computational power of direct simulation.

The computation field considered is a parallelepiped (fig.6) with the dimensions $L_x = 6b$, $L_y = 3b$ and $L_z = 4b$, where b is a characteristic dimension that corresponds to the separation distance between the counter-rotating vortices of the aircraft wake vortex.

The two counter-rotating vortices has been placed in the center of domain $x_{c_1} = 2.5b$, $x_{c_2} = 3.5b$, $y_{c_1} = y_{c_2} = 1.5b$.

We use a grid with $n_x = n_y = 256$ points and $n_z = 128$ points. The grid parameters of the computation field gives 8 388 608 computation cell. In the vortex longitudinal direction we use a regular grid with $dz = 0.0313$ ($r_0 / dz = 3.2$, where r_0 is the radius of core vortex, with $r_0 / b = 0.1$).

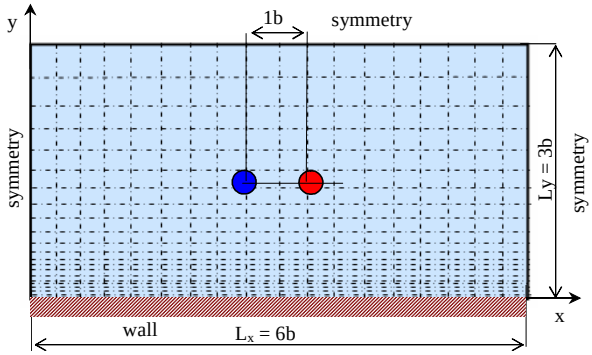

Fig. 5 Computation field and boundary conditions

In order to obtain a larger number of computation cell towards the vortices position and towards the wall, in the cross section we use an irregular grid. For the direction we use an irregular grid using an exponential law having near the wall the larger number of points.

The boundary conditions for the studied flow are the periodicity, symmetry and wall (fig. 5):

- In x direction we have assured care that the trajectories of the vortices are not too close to the boundary. In this direction we experience symmetry boundary conditions.
- In y direction we have wall boundary condition at the bottom and symmetry boundary condition at the top.
- Finally in the z direction, the axis of the vortex tubes, there are periodic conditions. We have chosen not to consider the long wavelength Crow instability for the main vortex tubes but to focus on the interaction with the wall and on the medium and short wavelength.

The initial conditions for the simulation (fig. 6) are the analytical solutions of an array of vortices images. The elementary vortex of this array is an Oseen vortex. A solitaire vortex is defined by its circulation Γ_0, and by its radius r_c corresponding of a maximal velocity. The position of the vortex center has been given by the coordinates (x_c, y_c) in the transverse plane (Oxy). Using a cylindrical system of coordinate (x, r, θ) whose origin is the vortex center, the rotation velocity $u_\theta(r)$ and the vorticity $\omega_x(r)$ of the vortex, are:

$$u_\theta(r) = \frac{\Gamma_0}{2\pi r}\left(1 - e^{-r^2/r_0^2}\right),\ \omega_x(r) = \frac{\Gamma_0}{\pi r_0^2} e^{-r^2/r_0^2}. \quad (11)$$

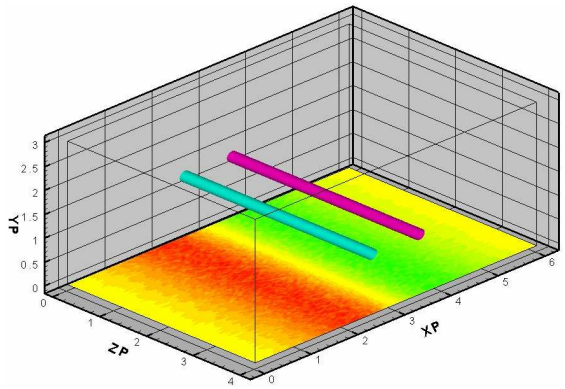

Fig. 8 The initial condition

For the dipole vortex, we use two longitudinal counter-rotating vortices described above, with the circulation $\Gamma_{01} = -\Gamma_0$, $\Gamma_{02} = \Gamma_0$, placed at distance b one from another (fig. 5). The referential parameters are the velocity and the time of descent of the vortices, the distance between the vortices and the Reynolds number:

$$U^* = \frac{\Gamma_0}{2\pi b};\ T^* = \frac{2\pi b^2}{\Gamma_0};\ L^* = b;\ \mathrm{Re} = \frac{\Gamma_0}{\nu}. \quad (12)$$

We obtain the following values: $U^* = 0.159$ m/s, $T^* = 6.28$ s and $\mathrm{Re} = 20000$. The initial velocity at each grid point is evaluated with the Biot-Savart law taking in account the boundary conditions and the infinite arrays of images. At initial iteration we introduce random perturbations for each 3 components of the velocity. The amplitude is equal to 10^{-2} times the maximum velocity in the field.

IV. Numerical results

The description of flow is based on the visualizations of fig. 7-14 and on the graph showing the distribution of the vorticity flux (fig. 16).

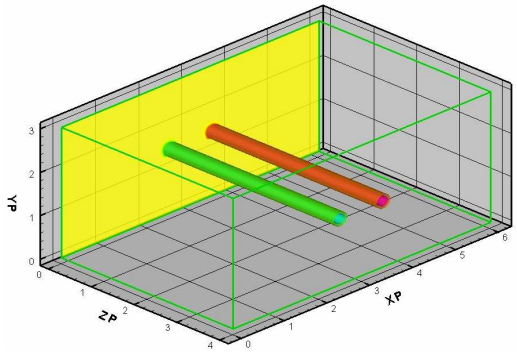

Fig.7 Visualization of the vorticity field (T=0)*

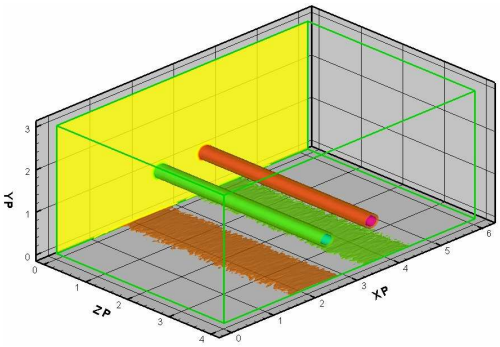

Fig.8 Visualization of the vorticity field (T=0.70)*

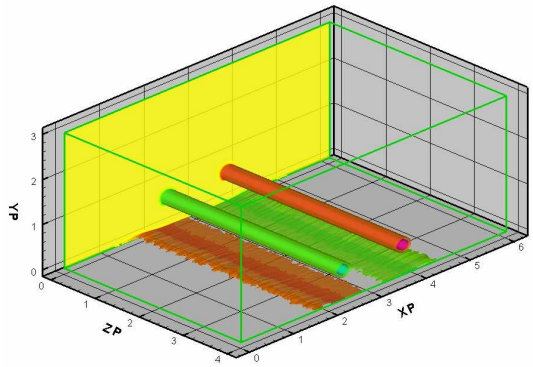

Fig.9 Visualization of the vorticity field (T=1.30)*

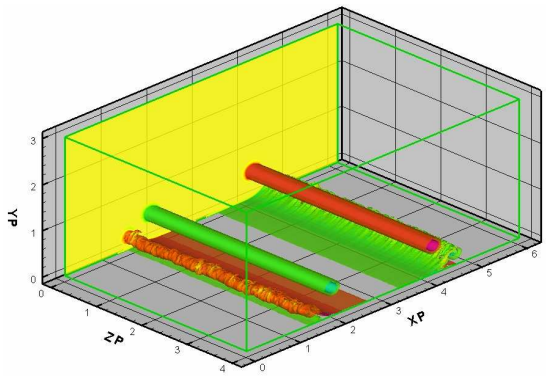

Fig.10 Visualization of the vorticity field (T=2.00)*

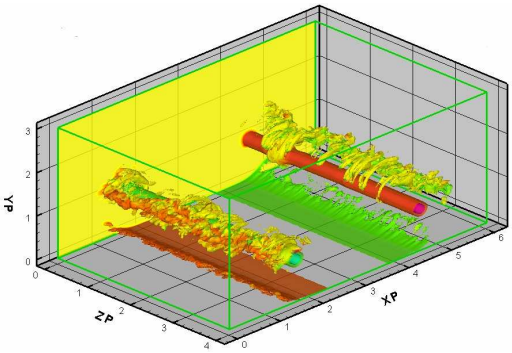

Fig.11 Visualization of the vorticity field (T=2.80)*

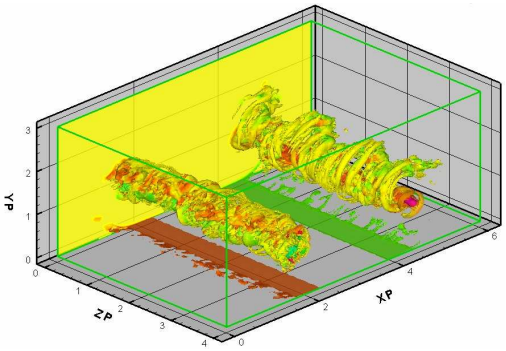

Fig.12 Visualization of the vorticity field (T=3.00)*

The fig. 9-14 visualize the vorticity field at different time steps using iso-surfaces of the axial vorticity ω_z. We notice at the beginning that the flow is 2D. The same a shear of vorticity appears near the wall.

When this shear of vorticity begins interacting with the main vortex, the vortices start to loose their coherence. The process begins by very short scale unsteadiness (length scale has the same order as the tube radius), which grows and produce streaks wrapped irregularly around the main vortex.

The production of small dissipative scales and the inter-diffusion at the periphery of the tube of opposite sign vorticity contribute to the weakening of the main vortices.

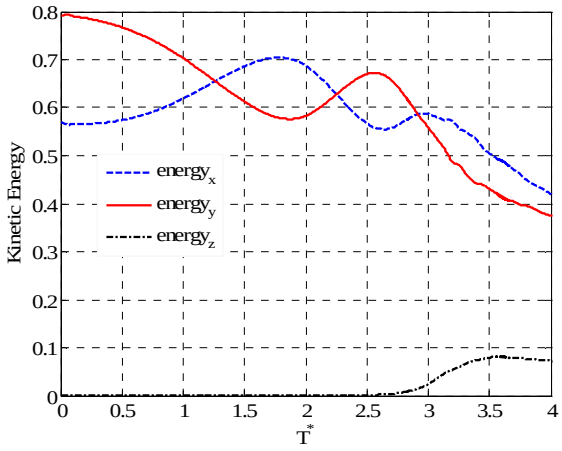

Fig.13 Distribution of the kinetic energy among the components of the velocity

The analysis of the vortex strength and its evolution with adimensional time are an important issue for the wake vortex hazard. We have considered different diagnostics as the kinetic energy (fig. 15), the enstrophy (fig.16) and the

evolution of the conventional value of the circulation Γ_{5-15} (fig. 17) and observed their time evolutions during the interaction process.

We notice that the creation of enstrophy (fig.16) by the small scales corresponds to a destruction of the kinetic energy (fig. 15).

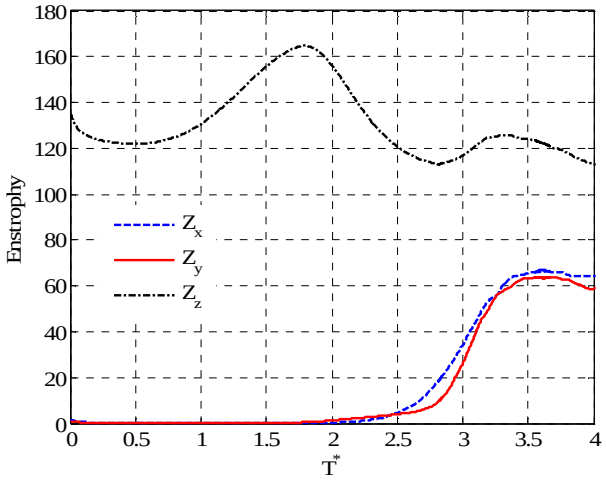

Fig.14 Distribution of the enstrophy among the components of the vorticity

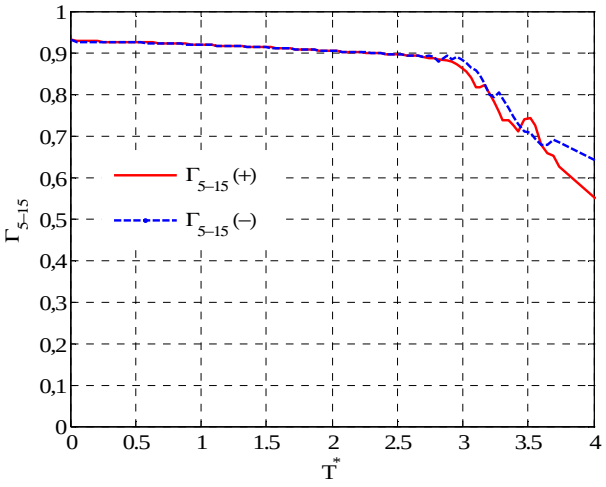

Fig.15 Time history of the circulation Γ_{5-15}

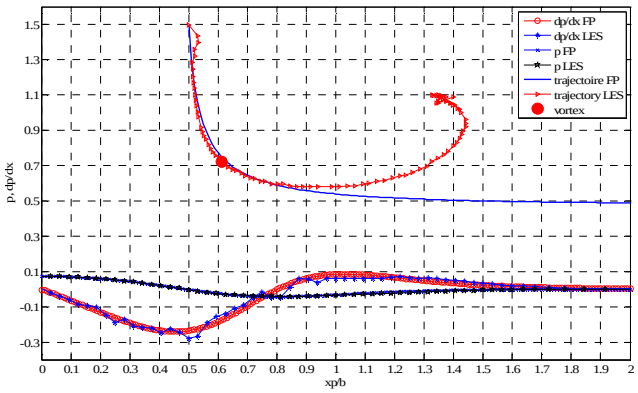

Fig.16 Distribution of the pressure and of the flux of vorticity

The evolution of the circulation Γ_{5-15} exhibits a decay at time $T^* = 3$. The key mechanism is the secondary vortex (see fig. 13) generated from the vorticity shear that wraps and loops around the main vortex and produces small scale unsteadiness. This is confirmed by energy and enstrophy diagnostics.

We obtained a distribution of the vorticity flux having a production of positive and negative vorticity (fig. 18). The pressure and vorticity distribution obtained by numerical simulation is similarly as the predicted distribution by theory study (fig. 3 and 4).

V. Conclusion

This study presents some results obtained by numerical simulation of a three dimensional wake vortex modelised by a pair of counter-rotating longitudinal vortices in interaction with a ground at a Reynolds number of 20000.

The post processing and the visualization give a good understanding of the behavior of the counter-rotating vortex pair in ground effect in terms of vortex dynamics all along the interaction. We have focused the analysis on the production of vorticity at the wall a concept proposed by Lighthill.

References

[1] PENEAU F., Etude numérique par simulation des grandes échelles de l'influence d'une forte turbulence extérieure sur les transferts pariétaux au sein d'une couche limite, PhD thesis, National Polytechnic Institute from Toulouse, France, 1999 ;

[2] MOLDOVEANU C., BOISSON H.C., GIOVANNINI A., Receptivity of a Longitudinal Contra-rotating Vortices Pair in an External Flow: a numerical experimentation, Congrès BAIL 2004, Toulouse, France, 5-9 juillet 2004 ;

[3] LIU, H.-T., Effects of Ambient Turbulence on the Decay of a Trailing Vortex, Journal of Aircraft, Vol. 29, No. 4, pp. 255-263, April 1992;

[4] CALMET I., MAGNAUDET J., Large eddy simulation of high-Schmidt number mass transfer in a turbulent channel flow, Phys. Fluids (9-2) pp. 438-455, 1996;

[5] SAFFMAN P.G., The approach of a vortex pair to a plane surface in an inviscid fluid, J. Fluid Mech. Vol 92 pp. 497-503, 1979;

[6] COTTET G.H. AND KOUMOUTSAKOS P., Vortex Methods; Theory and Practice, Cambridge University Press, 2000;

[7] PELLERIN S., Interaction d'une structure tourbillon avec une couche limite de plaque plane, Ph.D Thesis Paul Sabatier University, 1997 ;

[8] COTTIN, C., DUPONCHEEL, M., DAENINCK, G., LEWEKE, T., WINCKELMANS, G., Experimental and numerical study of counter-rotating vortex pair dynamics in ground effect, 18e Congrès Français de Mécanique, Grenoble, France 27-31 August 2007.